

# Long-term Proposal Report 1

## Nuclear Resonant Vibrational Spectroscopy for Observation of Fe-H/D Bending Modes in Hydrogenases and Nitrogenases

Cindy Pham<sup>1</sup>, Hongxin Wang<sup>1</sup>, Nakul Mishra<sup>1</sup>, Leland Gee<sup>1</sup>, Yoshitaka Yoda<sup>2</sup>, Thomas B. Rauchfuss<sup>3</sup>, Vladimir Pelmeshnikov<sup>4</sup>, Hideaki Ogata<sup>5</sup>, Edward J. Reijerse<sup>5</sup>, Wolfgang Lubitz<sup>5</sup>, Nimesh Khadka<sup>6</sup>, Lance Seefeldt<sup>6</sup>, Stephen P. Cramer<sup>1</sup>

<sup>1</sup>Department of Chemistry, University of California, Davis, CA, USA

<sup>2</sup>Research & Utilization Division, JASRI, SPring-8, Japan

<sup>3</sup>Department of Chemistry, University of Illinois, Urbana, IL, USA

<sup>4</sup>Department of Chemistry, Technische Universität Berlin, Berlin, Germany

<sup>5</sup>Max Plank Institute for Chemical Energy Conversion, Muelheim an der Ruhr, Germany

<sup>6</sup>Department of Chemistry and Biochemistry, Utah State University, Salt Lake City, UT, USA

### Abstract

Using <sup>57</sup>Fe nuclear resonant vibrational spectroscopy (NRVS), we have characterized several important <sup>57</sup>Fe-labeled proteins such as [FeFe] hydrogenase ([FeFe] H<sub>2</sub>ase), [NiFe] hydrogenase ([NiFe] H<sub>2</sub>ase), and nitrogenase (N<sub>2</sub>ase). Following the successful observation of the Ni-H-Fe wag mode in *Desulfovibrio vulgaris* Miyazaki F [NiFe] H<sub>2</sub>ase (*DvMF* for abbreviation), we extended these studies to other enzymes, such as *Chlamydomonas reinhardtii* [FeFe] H<sub>2</sub>ase (*Cr-HydA1*) and *Desulfovibrio desulfuricans* [FeFe] H<sub>2</sub>ase (*Dd-HydAB*). Fe-hydride and Fe-deuteride related bending modes in [FeFe] H<sub>2</sub>ases were observed and interpreted by density functional theory (DFT) calculations. We also observed the interaction between the amine group (NH) in the azadithiolate (ADT) bridge and the Fe-H/D structure by comparing the *wild type Dd-HydAB* result with that from a variant with an oxodithiolate (ODT) bridge. With the advancement we have made for studying H<sub>2</sub>ase, we have also better characterized the catalytic intermediates in N<sub>2</sub>ase, such as the E<sub>4</sub> state.

### Background and Purpose

H<sub>2</sub>ases catalyze the reversible reaction of  $2\text{H}^+ + 2\text{e}^- \rightleftharpoons \text{H}_2$ <sup>[1-3]</sup>, while N<sub>2</sub>ases catalyze the fixation of molecular nitrogen (N<sub>2</sub>) in the atmosphere into bio-available NH<sub>3</sub><sup>[4,5]</sup>. Since today's world faces multiple pressures from the demands for sustainable energy and food resources, H<sub>2</sub>ases and N<sub>2</sub>ases have both attracted a lot of attention and have been intensively studied for decades. Although crystal structures are available for all of these enzymes (Figure 1), many key enzyme intermediates cannot be crystallized. We are therefore using spectroscopy as an alternative probe of these key intermediates, with the overarching goal of understanding the catalytic mechanisms of these systems.

Nuclear resonant vibrational spectroscopy (NRVS)

measures vibrational transitions that occur together with nuclear transitions that are typically associated with the Mossbauer effect<sup>[6,9]</sup>. For the study of Fe in biology, <sup>57</sup>Fe NRVS has key features that complement traditional techniques such as infrared (IR) and Raman spectroscopies. Despite the complexity of these samples, <sup>57</sup>Fe NRVS only sees normal modes that involve motion of the <sup>57</sup>Fe nucleus. Since the NRVS intensity is proportional to this <sup>57</sup>Fe motion, the NRVS spectrum is easy to calculate from a normal mode analysis of a candidate structure. The technique has moderate sensitivity, and at the moment can be used to study frozen protein samples at ~mM concentrations<sup>[9,10]</sup>. Over the past decade, this technique has been used to study the lower frequency modes of a wide variety of Fe complexes and proteins<sup>[11-14]</sup>. More recently, we

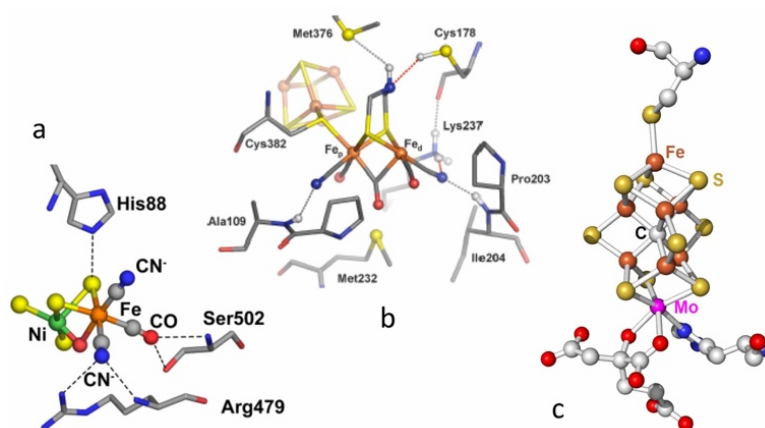


Figure 1 Crystal structures of the catalytic centers: (a) [NiFe] center inside a typical [NiFe] H<sub>2</sub>ase; (b) H cluster inside a typical [FeFe] H<sub>2</sub>ase; (c) FeMo cofactor inside a typical N<sub>2</sub>ase.

have extended NRVS studies to more difficult Fe-H related vibrational features in several H<sub>2</sub>ase enzymes as will be detailed later in this article<sup>[14]</sup>.

Our NRVS measurements were performed at SPring-8 BL09XU<sup>[15]</sup>, which uses a high heat load monochromator to produce 14.4 keV radiation with  $\sim 1.0$  eV resolution, followed by a Ge(422)  $\times$  2Si(975) high energy resolution monochromator (HRM) to narrow the resolution to  $\sim 0.8$  meV, with a final flux of  $\sim 2.5 \times 10^9$  photons/s. Some NRVS data were also measured at SPring-8 BL19LXU. The NRVS measurements used a  $2 \times 2$  avalanche photodiode (APD) detector array to collect the nuclear fluorescence and the internal conversion Fe K $\alpha$  fluorescence following <sup>57</sup>Fe nuclear excitation. The typical background count rates for this array is  $\sim 0.03$  cts/s<sup>-1</sup>. A closed-cycle liquid helium flow cryostat was used to maintain the samples at cryogenic temperatures ( $\sim 50$  K). During the NRVS measurements, the scans were often divided into segments with different data collection times at a given energy. These acquisition times ranged from 1-3 s in the Fe-S region to as much as 30 s per point for weak Fe-H related modes. The energy scale was always calibrated with respect to a standard sample of [<sup>57</sup>FeCl<sub>4</sub>][NEt<sub>4</sub>], which has a prominent peak at 380 cm<sup>-1</sup>. Raw NRVS data were converted to PVDOS using the PHOENIX software package<sup>[7]</sup>.

## Results

### [NiFe] H<sub>2</sub>ases

The crystal structure for the [NiFe] center in *Desulfovibrio vulgaris* Miyazaki F [NiFe]-H<sub>2</sub>ase (DvMF) is shown as in Figure 1a. By a series of careful and strenuous NRVS measurements, we recorded the first direct spectroscopic

evidence for a bridging Ni-H-Fe species in a <sup>57</sup>Fe-labeled DvMF Ni-R sample. The overall NRVS spectra are shown as in Figure 2, with Fe-S, Fe-CN/CO and the weak Ni-H-Fe features. Via DFT simulation on the measured PVDOS, the optimized structure with detailed H and S bonding information (Figure 2, insert) was obtained as the possible Ni-R structural candidate. The biochemical science and the DFT simulations were presented and well-discussed in an article in *Nature Communications* in 2015<sup>[14]</sup>, while its technical details leading to the successful observation of the weak Ni-H-Fe wag mode was presented in *J. Synchrotron Rad* in the same year<sup>[16]</sup>.

The existence of Ni-H-Fe in DvMF Ni-R has provided a critical reference for the DFT simulation to determine the possible Ni-R structure (Figure 2, insert). The successful observation of this extremely weak feature also has: 1) established that a 0.1 cts/s<sup>-1</sup> Fe-H related bending/wagging mode is observable although it has a much weaker NRVS

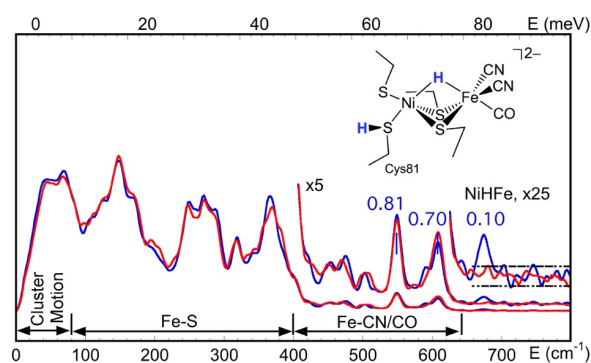


Figure 2 PVDOS of DvMF Ni-R prepared under H<sub>2</sub>/H<sub>2</sub>O (—) and D<sub>2</sub>/D<sub>2</sub>O (—) conditions. The blue numbers are the NRVS signal levels for the corresponding Fe-CO and Ni-H-Fe features; (insert) the best Ni-R structural model obtained from DFT simulation of the PVDOS.

signal than the already weak Fe-CO<sup>[14,17,18]</sup>; 2) identified the energy position for the Ni-H-Fe at 675 cm<sup>-1</sup>, which was virtually unknown because this position is much lower than the Fe-H bending positions in model complexes or in previous DFT “predictions”; 3) demonstrated that the comparison of Fe-CO features in H<sub>2</sub>/H<sub>2</sub>O (—) vs. D<sub>2</sub>/D<sub>2</sub>O (—) prepared Ni-R samples can also be used as an indirect evidence for the existence of Ni-H-Fe in addition to the direct observation.

[FeFe] H<sub>2</sub>ases

We then successfully evaluated two H<sub>2</sub>/H<sub>2</sub>O vs. D<sub>2</sub>/D<sub>2</sub>O [FeFe] H<sub>2</sub>ase enzyme pairs from the *Chlamydomonas reinhardtii* [FeFe] H<sub>2</sub>ase (*Cr-HydA1*) and the *Desulfovibrio desulfuricans* [FeFe] H<sub>2</sub>ase (*Dd-HydAB*). *Dd-HydAB* differs

from *Cr-HydA1* by the amount of [4Fe4S] accessory clusters in the enzyme, but their active sites are the same - both consist of a binuclear Fe-S subcluster ([2Fe]<sub>H</sub>) bound to a special [4Fe4S]<sub>H</sub> cluster via a cysteine to form an H-cluster (as illustrated in Figure 1b).

First, a synthetic precursor [57Fe<sub>2</sub>(adt)(CN)<sub>2</sub>(CO)<sub>4</sub>]<sup>2-</sup> (where adt<sup>2-</sup>=[(SCH<sub>2</sub>)<sub>2</sub>NH]<sup>2-</sup>) was produced and artificially inserted into the Apo-*Cr-HydA1* enzyme (Figure 3a). This approach allows for the specific <sup>57</sup>Fe labeling of the [2<sup>57</sup>Fe]<sub>H</sub> subcluster, while leaving other irons unlabeled. The PVDOS for such labeled *Cr-HydA1* Hox-CO (—) and its precursor (—) were observed as shown in Figure 4a, from which we identified Fe-S modes from 0 to 300 cm<sup>-1</sup>, 2 Fe-CN modes at 400-450 cm<sup>-1</sup>, and 6 Fe-CO modes at 480-700 cm<sup>-1</sup>. This labeling has helped

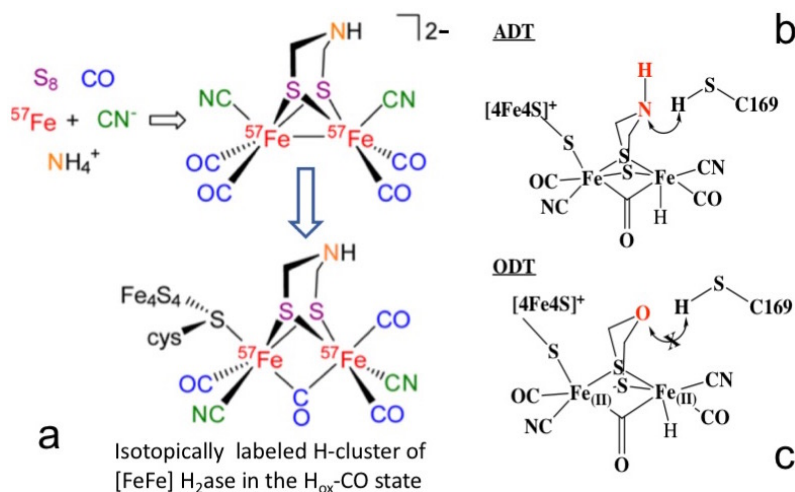


Figure 3 (a) The artificial maturation process of [FeFe] H<sub>2</sub>ase using a [57Fe<sub>2</sub>(adt)(CN)<sub>2</sub>(CO)<sub>4</sub>]<sup>2-</sup> precursor<sup>[19]</sup>; (b, c) manipulation of the active sites from ADT (b, with a NH) to ODT (c, with an O)<sup>[21]</sup>.

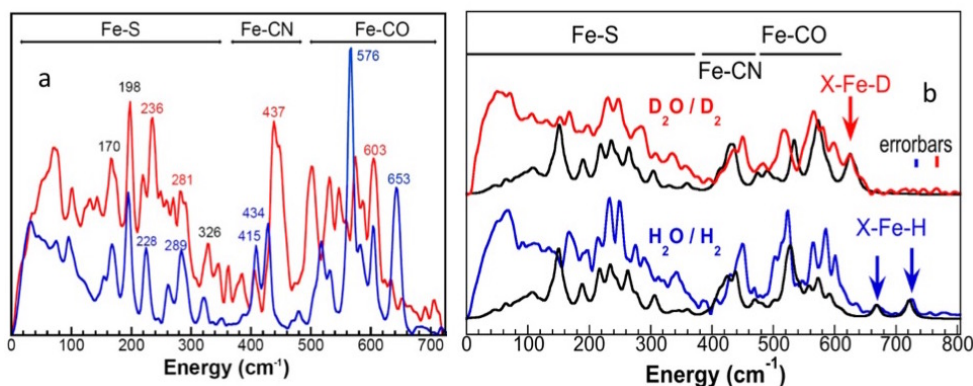


Figure 4 (a) PVDOS of <sup>57</sup>Fe-labeled [2Fe]<sub>H</sub> subcluster in *HydA1* Hox-CO (—) and the precursor [57Fe<sub>2</sub>(adt)(CN)<sub>2</sub>(CO)<sub>4</sub>]<sup>2-</sup> (—). Important peak positions are labeled in the color corresponding to the spectra, or in black while the positions are the same for both spectra<sup>[19]</sup>; (b) the observed PVDOS spectra for *Cr*-ODT prepared under D<sub>2</sub>/D<sub>2</sub>O (—) vs. under H<sub>2</sub>/H<sub>2</sub>O (—) conditions vs. the DFT calculations (—). The arrows indicate the X-Fe-H/D bending features.

characterize key intermediates in the catalytic cycle and advanced our spectroscopic investigation of [FeFe] H<sub>2</sub>ases.

Taking advantage of the same protocol, we successfully replaced the azadithiolate (ADT) bridge of the active site in *Cr-HydA1* (Figure 3b) with an oxodithiolate (ODT) bridge (or NH→O) to form an ODT variant (*Cr*-ODT, Figure 3c)<sup>[19]</sup>. This replacement obstructs the proton transport chain, which allows us to trap a transient intermediate (known as the H<sub>hyd</sub> state)<sup>[20]</sup> with high population.

For *Cr*-ODT (Figure 3c), we have observed clear Fe-H/D bending features (Figure 4b). The H<sub>2</sub>/H<sub>2</sub>O prepared sample leads to a well-resolved band at 727 cm<sup>-1</sup> (in-plane bending mode) and a smaller feature at 670 cm<sup>-1</sup> (out-of-plane wagging mode) (Figure 4b, —). Its X-Fe-H wagging mode has a similar energy position as the Ni-H-Fe wagging mode in *Dv*MF Ni-R (Figure 2, at 675 cm<sup>-1</sup>). The sample prepared under D<sub>2</sub>/D<sub>2</sub>O does not have these features, but instead shows a sharp peak at 625 cm<sup>-1</sup>; the second Fe-D band is presumably highly mixed with Fe-CO features (Figure 4b, —). The observed H/D-dependent spectral changes in the 400-800 cm<sup>-1</sup> region coupled

with the <sup>57</sup>Fe-H/D DFT calculations clearly confirmed our mode assignments. Using observed PVDOS and DFT simulations, we have concluded the strong evidence for the X-Fe-H related modes in transient states of H<sub>hyd</sub> in *Cr*-ODT, which has a similar NRVS signal level with *Dv*MF Ni-R (both at ~0.1 cts/s<sup>-1</sup>).

In addition to observing the transient intermediate in *Cr*-ODT, we were also able to observe a catalytic intermediate in the *wild type Dd-HydAB* (with an ADT bridge, PVDOS not shown). Direct evidence for the terminal Fe-H bending mode has led to the identification of the intermediate H<sub>hyd</sub> and the difference between *Cr*-ODT and *Dd-HydAB* has helped understand of the interaction between the amine group (NH) and the terminal Fe-H structure in the catalytic cycle.

#### N<sub>2</sub>ases

We also evaluated the E<sub>4</sub> state in V70I variant of the N<sub>2</sub>ase. This so-called Janus intermediate is considered to be the turning point in the biological nitrogen fixation mechanism (Figure 5). The intermediate was freeze-trapped with high populations

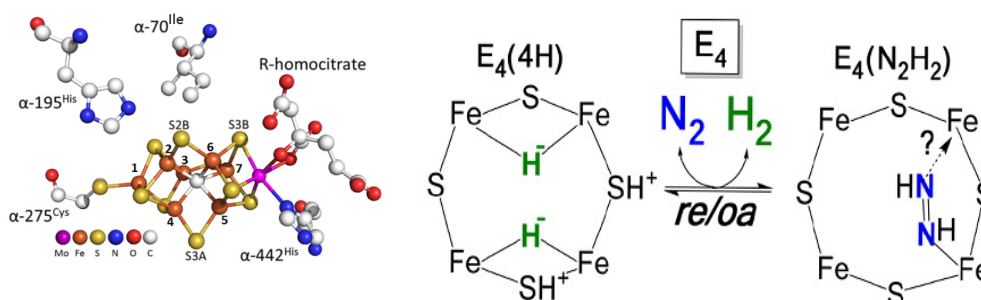


Figure 5 (a) Local structure around the active site (FeMo-cofactor) in V70I mutant Av N<sub>2</sub>ase<sup>[22]</sup>, (b) proposed mechanistic pathway of nitrogen binding at E<sub>4</sub> intermediate step<sup>[23,24]</sup>.

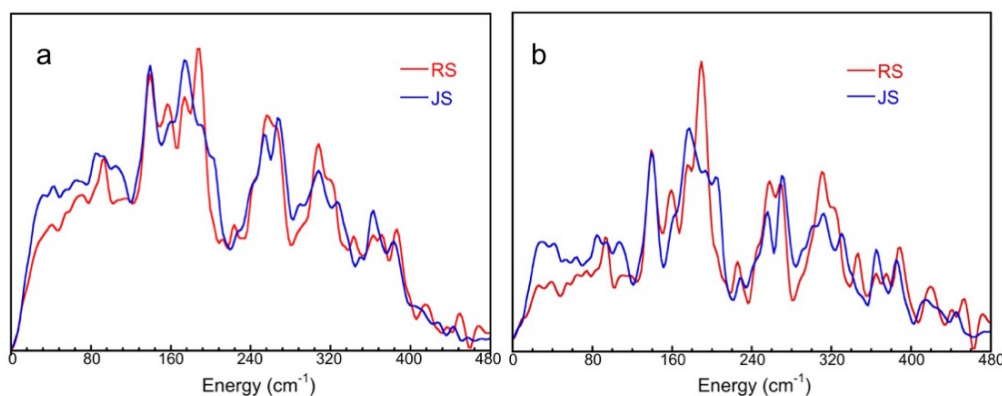


Figure 6 The <sup>57</sup>Fe PVDOS of Av N<sub>2</sub>ase MoFe protein (a) and of FeMo-co inside it (b) for JS (—) vs. RS (—).

from the *Azotobacter vinelandii* (Av) strains. The resting state (RS, E<sub>0</sub>), the Janus intermediate (JS, E<sub>4</sub>) were prepared in H<sub>2</sub>O and D<sub>2</sub>O buffers, respectively.

Figure 6a compares the <sup>57</sup>Fe PVDOS for the RS and JS V70I variant of N<sub>2</sub>ase in D<sub>2</sub>O. N<sub>2</sub>ase MoFe protein consists FeMo-cofactor (FeMo-co, 7Fe) and P-cluster (8Fe). We are able to obtain the PVDOS for FeMo-co by subtracting the PVDOS for *nifE* (containing only P-cluster) from the PVDOS of the whole MoFe protein. The FeMo-co PVDOS for RS and JS are shown as in Figure 6b. The PVDOS for RS is dominated by a peak near 188 cm<sup>-1</sup> with a resolved shoulder at 172 cm<sup>-1</sup> (Figure 6a, b, —). This mode has been associated with the ‘breathing’ mode of the FeMo cofactor which involves expansion and contraction of the [6Fe–C] core<sup>[13,25]</sup>. The spectrum for JS shows a diminished intensity at this peak (Figure 6a, b, —).

The above illustration (Figure 6) is indirect evidence for the Fe-D bonding, which is consistent with our previous observation on the CO bound Av N<sub>2</sub>ase PVDOS<sup>[13]</sup>. Preliminary direct evidence for Fe-D and Fe-H interactions were also observed and the corresponding DFT simulations are underway.

## Summary

In the last long term proposal (2013B0103-2016A0103) at SPring-8 BL09XU, and in combination with some work from BL19LXU, we have obtained significant NRVS results for many important enzymes. One of the most important results is our observation of Fe-H/D bending modes in NRVS for H<sub>2</sub>ases. Improvements of the SPring-8 synchrotron light source, beamline monochromators, and detectors have allowed us to measure these extremely weak features with NRVS. The results for [FeFe] H<sub>2</sub>ase, [NiFe] H<sub>2</sub>ase, and N<sub>2</sub>ase will allow chemists to better understand H interaction in these important enzymes. Moving forward, we hope to be able to push the NRVS observation to higher energy regions and to resolve the Fe-H/D stretching modes for the appropriate enzymes. In addition, we also hope to combine multiple experimental methods with NRVS, e.g. photolysis NRVS and/or NRVS/IR simultaneous measurements, which will be a great addition to our tool box to analyze critical intermediates in the enzymatic catalysis.

## Acknowledgments

We thank Dr. Kenji Tamasaku very much for his assistance in our beamtime at BL19LXU and other contributions.

This work was supported by NIH grant GM-65440 (to S.P.C.). V.P. was supported by UniCat initiative of DFG.

## References

- [ 1 ] Kim, J. Y. H. and Cha, H. J.: *Korean Journal of Chemical Engineering* **2013**, *30*, 1-10.
- [ 2 ] Jugder, B. E.; Welch, J.; Aguey-Zinsou, K. F. and Marquis, C. P.: *Rsc Advances* **2013**, *3*, 8142-8159.
- [ 3 ] Lubitz, W.; Ogata, H.; Rüdiger, O. and Reijerse, E.: *Chem Rev* **2014**, *114*, 4081-4148.
- [ 4 ] Spatzal, T.; Schlesier, J.; Burger, E.-M.; Sippel, D.; Zhang, L.; Andrade, S. L. A.; Rees, D. C. and Einsle, O.: *Nature Comm.* **2016**, *7*, 10902.
- [ 5 ] Hoffman, B. M.; Lukoyanov, D.; Dean, D. R. and Seefeldt, L. C.: *Acc. Chem. Res.* **2013**, *46*, 587-595.
- [ 6 ] Seto, M.; Yoda, Y.; Kikuta, S.; Zhang, X. W. and Ando, M.: *Phys Rev Lett* **1995**, *74*, 3828.
- [ 7 ] Sturhahn, W.; Toellner, T. S.; Alp, E. E.; Zhang, X.; Ando, M.; Yoda, Y.; Kikuta, S.; Seto, M.; Kimball, C. W. and Dabrowski, B.: *Physical Review Letters* **1995**, *74*, 3832-3835.
- [ 8 ] Yoda, Y.; Okada, K.; Wang, H.; Cramer, S. P. and Seto, M.: *Japanese Journal of Applied Physics* **2016**, *55*, 122401.
- [ 9 ] Wang, H.; Alp, E. E.; Yoda, Y. and Cramer, S. P.: *Methods in Molecular Biology; Metalloproteins: Methods and Protocols* **2014**, *1122*, 125-137.
- [10] Smith, M. C.; Xiao, Y.; Wang, H.; George, S. J.; Coucovanis, D.; Koutmos, M.; Sturhahn, W.; Alp, E. E.; Zhao, J. and Cramer, S. P.: *Inorg. Chem.* **2005**, *44*, 5562-5570.
- [11] Serrano, P. N.; Wang, H.; Crack, J. C.; Prior, C.; Hutchings, M. I.; Thomson, A. J.; Kamali, S.; Yoda, Y.; Zhao, J.; Hu, M. Y.; Alp, E. E.; Oganessian, V. S.; Le Brun, N. E. and Cramer, S. P.: *Angewandte Chemie International Edition* **2016**, *55*, 14575-14579.
- [12] Cramer, S. P.; Xiao, Y.; Wang, H.; Guo, Y. and Smith, M. C.: *Hyp. Interact.* **2006**, *170*, 47.
- [13] Scott, A.; Pelmenchikov, V.; Guo, Y.; Yan, L.; Wang, H.; George, S. J.; Dapper, C. H.; Newton, W. E.; Yoda, Y.; Tanaka, Y. and Cramer, S. P.: *Journal of the American Chemical Society* **2014**, *136*, 15942-15954.
- [14] Ogata, H.; Krämer, T.; Wang, H.; Schilter, D.; Pelmenchikov, V.; van Gastel, M.; Neese, F.; Rauchfuss, T. B.; Gee, L. B.; Scott, A. D.; Yoda, Y.; Tanaka, Y.; Lubitz, W. and Cramer, S. P.: *Nature Comm.* **2015**, *6*, 7890.
- [15] Yoda, Y.; Yabashi, M.; Izumi, K.; Zhang, X. W.; Kishimoto, S.; Kitao, S.; Seto, M.; Mitsui, T.; Harami, T.; Imai, Y. and Kikuta, S.: *Nuclear Instruments & Methods in*

- Physics Research Section A-Accelerators Spectrometers Detectors & Associated Equipment* **2001**, *467*, 715-718.
- [16] Wang, H.; Yoda, Y.; Ogata, H.; Tanaka, Y. and Lubitz, W.: *Journal of Synchrotron Radiation* **2015**, *22*, 1334-1344.
- [17] Pelmenchikov, V.; Guo, Y.; Wang, H.; Cramer, S. P. and Case, D. A.: *Faraday Discussions* **2011**, *148*, 409-420.
- [18] Kamali, S.; Wang, H.; Mitra, D.; Ogata, H.; Lubitz, W.; Manor, B. C.; Rauchfuss, T. B.; Byrne, D.; Bonnefoy, V.; Jenney Jr., F. E.; Adams, M. W. W.; Yoda, Y.; Alp, E.; Zhao, J. and Cramer, S. P.: *Angewandte Chemie-International Edition* **2013**, *52*, 724-728.
- [19] Gilbert-Wilson, R.; Siebel, J. F.; Adamska-Venkatesh, A.; Pham, C. C.; Reijerse, E.; Wang, H.; Cramer, S. P.; Lubitz, W. and Rauchfuss, T. B.: *Journal of the American Chemical Society* **2015**, *137*, 8998-9005.
- [20] Long, H.; King, P. W. and Chang, C. H.: *J Phys Chem B* **2014**, *118*, 890-900.
- [21] Reijerse, E. J.; Pham, C. C.; Pelmenchikov, V.; Gilbert-Wilson, R.; Adamska-Venkatesh, A.; Siebel, J. F.; Gee, L. B.; Yoda, Y.; Tamasaku, K.; Lubitz, W.; Rauchfuss, T. B. and Cramer, S. P.: *J Amer Chem Society* accepted March 13, **2017**. (doi:10.1021/jacs.7b00686)
- [22] Spatzal, T.; Aksoyoglu, M.; Zhang, L.; Andrade, S. L. A.; Schleicher, E.; Weber, S.; Rees, D. C. and Einsle, O.: *Science* **2011**, *334*, 940.
- [23] Lukoyanov, D.; Yang, Z. Y.; Khadka, N.; Dean, D. R.; Seefeldt, L. C. and Hoffman, B. M.: *Journal of the American Chemical Society* **2015**, *137*, 3610-3615.
- [24] Yang, Z. Y.; Khadka, N.; Lukoyanov, D.; Hoffman, B. M.; Dean, D. R. and Seefeldt, L. C.: *Proc. Natl. Acad. Sci. U. S. A.* **2013**, *110*, 16327-16332.
- [25] Xiao, Y.; Fisher, K.; Smith, M. C.; Newton, W. E.; Case, D. A.; George, S. J.; Wang, H.; Sturhahn, W.; Alp, E. E.; Zhao, J.; Yoda, Y. and Cramer, S. P.: *Journal of the American Chemical Society* **2006**, *128*, 7608-7612.